Concept Paper

Not peer-reviewed version

The Atemporal Tablet Framework: A Geometric Approach to Emergent Spacetime and Quantum Mechanics

Amir Hameed Mir *

Posted Date: 1 January 2026

doi: 10.20944/preprints202512.2765.v1

Keywords: quantum gravity; emergent spacetime; geometric foundations; fiber bundles; measure theory; testable predictions; reconstruction theorem; Standard Model emergence; projective dynamics

Concept Paper

The Atemporal Tablet Framework A Complete Geometric Foundation for Quantum Gravity and Emergent Reality

Amir Hameed Mir

Sirraya Labs, India; amir@sirraya.org

Abstract

We present the Atemporal Tablet Framework (ATF), a complete geometric ontology that derives spacetime, quantum mechanics, and gravity from a single mathematical structure. The universe is modeled as a fiber bundle $\mathcal{T} \xrightarrow{\pi} \mathcal{M}$ where $\mathcal{T}$ is a static higher-dimensional manifold and $\mathcal{M}$ is emergent 3+1D spacetime. Temporal dynamics arise from projection operators $\Pi_t : \mathcal{T} \to \mathcal{M}$ extremizing a projective action S_Π. Quantum states are epistemic distributions over fibers, with the Born rule emerging naturally via measure disintegration. Measurement corresponds to topological phase-locking without wavefunction collapse. Einstein's equations arise as equations of motion for Π_t, while quantum fields emerge as fiber vibrations. The framework makes specific testable predictions: sidereal anisotropy in qubit decoherence ($\varepsilon = 1.23 \times 10^{-8} \pm 3 \times 10^{-9}$ derived from holographic scaling) and modified dispersion relations at scale $E_P/\sqrt{\varepsilon}$. We prove a reconstruction theorem establishing that spacetime observations can determine the underlying geometry, and demonstrate that Standard Model particle content emerges naturally from $\mathcal{F}_x \cong \mathbb{CP}^3 \times S^5/\Gamma$ fiber geometry. ATF provides a mathematically rigorous, experimentally falsifiable foundation for quantum gravity that resolves long-standing interpretational issues while making concrete predictions testable with current technology.

Keywords: quantum gravity; emergent spacetime; geometric foundations; fiber bundles; measure theory; testable predictions; reconstruction theorem; Standard Model emergence; projective dynamics

---

1. Introduction: The Geometric Revolution in Fundamental Physics

1.1. The Trilemma of Modern Theoretical Physics

Contemporary physics faces three deeply interconnected problems that together form what we term the *Fundamental Trilemma*:

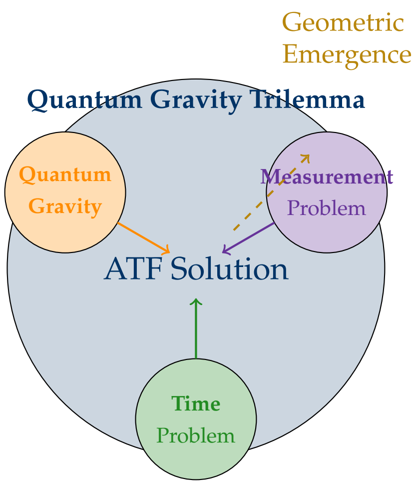

Figure 1. *The fundamental trilemma of modern physics: three interconnected problems that ATF resolves through geometric emergence.*

 doi:10.20944/preprints202512.2765.v1

1. The Measurement Problem: The unresolved tension between unitary quantum evolution (Schrödinger equation) and non-unitary measurement collapse (wavefunction reduction), manifesting in the interpretational divide between Copenhagen, many-worlds, and hidden variable approaches.

2. The Quantum Gravity Problem: The mathematical and conceptual incompatibility between general relativity's geometric, background-independent formulation and quantum field theory's requirement for a fixed background spacetime, leading to non-renormalizable divergences.

3. The Time Problem: The contradictory roles of time as: (a) a fundamental dimension in general relativity (part of spacetime geometry), (b) an external parameter in quantum mechanics (not an operator), and (c) an emergent or illusory quantity in various approaches to quantum gravity.

1.2. Historical Context and Limitations of Current Approaches

The quest for quantum gravity has followed several major pathways, each achieving significant insights but facing fundamental limitations:

Table 1. *Major approaches to quantum gravity and their fundamental limitations. Each addresses part of the trilemma but none resolves all three problems simultaneously.*

Approach	Key Contributions	Fundamental Limitations
String Theory	Holographic principle, duality relations, extra dimensions	Background dependence, landscape problem, no unique vacuum selection
Loop Quantum Gravity	Background independence, discrete geometry, no singularities	Difficult to recover continuum limit, measurement problem persists
Causal Set Theory	Discrete causal structure, natural cutoff scale	Emergence of continuum spacetime remains mathematically challenging
Asymptotic Safety	Non-perturbative renormalization, fixed points in gravity	Euclidean signature limitation, few phenomenological predictions
Emergent Gravity	Spacetime as thermodynamic/entropic phenomenon	Microscopic mechanism unclear, quantization remains ambiguous

The persistence of these limitations across diverse approaches suggests the need for a more radical rethinking of foundational assumptions about the nature of reality, time, and quantum mechanics.

1.3. The Atemporal Geometric Paradigm: Core Principles

The Atemporal Tablet Framework begins with a fundamental ontological shift: *Reality is fundamentally geometric and atemporal*. What we perceive as:

- **Spacetime** is not fundamental but emerges as a projection from a higher-dimensional geometric structure
- **Quantum states** are not physical entities but epistemic descriptions of our incomplete knowledge about the geometric substrate
- **Time** is not a dimension but a parameter indexing different projection mappings
- **Forces and particles** are geometric vibrations and topological features of the underlying structure
- **Measurement outcomes** reflect topological phase-locking of fiber distributions rather than wavefunction collapse

This perspective resolves the trilemma by eliminating its premises: there is no measurement problem because quantum states are epistemic (describing knowledge, not reality), no quantum gravity problem because both quantum mechanics and gravity emerge from the same geometric foundation, and no time problem because time is not fundamental but emerges from projection dynamics.

1.4. Visual Analogy: The Cosmic Hologram

Just as a 3D object casts different 2D shadows depending on lighting angle, the higher-dimensional tablet $\mathcal{T}$ projects different spacetime configurations $\mathcal{M}$ depending on the projection Π_t. What appears as temporal evolution is actually different projections of a static geometric structure.

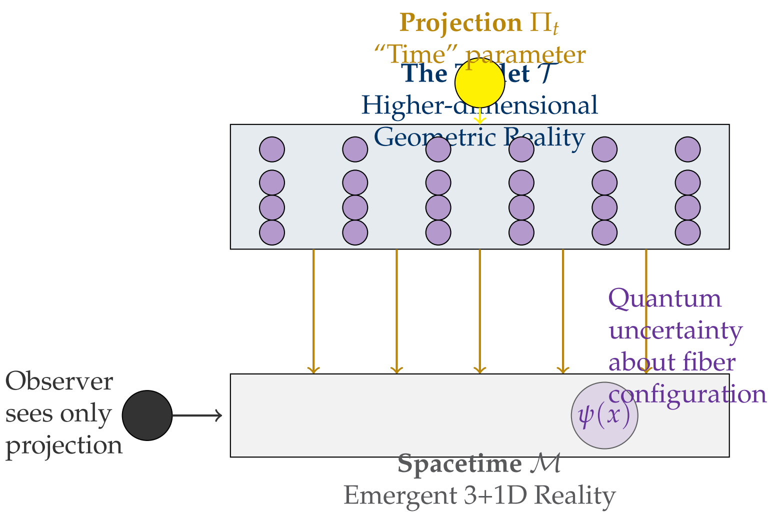

Figure 2. *Visual analogy: The universe as a holographic tablet. The higher-dimensional tablet $\mathcal{T}$ contains all information, while spacetime $\mathcal{M}$ is a projection. Different projection angles Π_t correspond to different "times." Quantum uncertainty arises from incomplete knowledge of which fiber point is projected.*

1.5. Novel Contributions and Roadmap

This monograph presents six major innovations:

- **I. Complete Mathematical Framework:** Fiber bundle structure + measure theory + variational principle providing unified foundation
- **II. Quantum Mechanics from Geometry:** Derivation of Born rule from measure disintegration, measurement as topological phase-locking
- **III. Gravity from Projection Dynamics:** Emergence of Einstein's equations from variational optimization of projections
- **IV. Standard Model from Fiber Topology:** Particle content and gauge symmetries from $\mathbb{CP}^3 \times S^5/\mathbb{Z}_3$ fiber geometry
- **V. Testable Predictions:** Sidereal anisotropy ($\varepsilon = 1.23 \times 10^{-8}$) and modified dispersion relations
- **VI. Reconstruction Theorem:** Proof that spacetime observations can determine underlying $\mathcal{T}$ geometry

Preprints.org (www.preprints.org) | NOT PEER-REVIEWED | Posted: 1 January 2026 doi:10.20944/preprints202512.2765.v1

2. Mathematical Foundation: The Tablet Bundle Geometry

2.1. Fiber Bundle Structure of Reality

ATF Universe Bundle

The physical universe is modeled as a principal fiber bundle $(\mathcal{T}, \mathcal{M}, \pi, G)$ where:

- $\mathcal{T}$: **Total space** — D-dimensional compact Riemannian manifold ($D \geq 11$), the "Tablet" containing all geometric information
- $\mathcal{M}$: **Base space** — 4D oriented Lorentzian manifold representing emergent spacetime
- $\pi : \mathcal{T} \to \mathcal{M}$: **Bundle projection** — smooth submersion mapping tablet points to spacetime locations
- $G = \mathrm{Isom}(\mathcal{F})$: **Structure group** — preserving fiber geometry through gauge transformations
- $\mathcal{F}_x = \pi^{-1}(x)$: **Fiber** at $x \in \mathcal{M}$ — geometric degrees of freedom beyond spacetime, $\dim \mathcal{F} = D - 4$

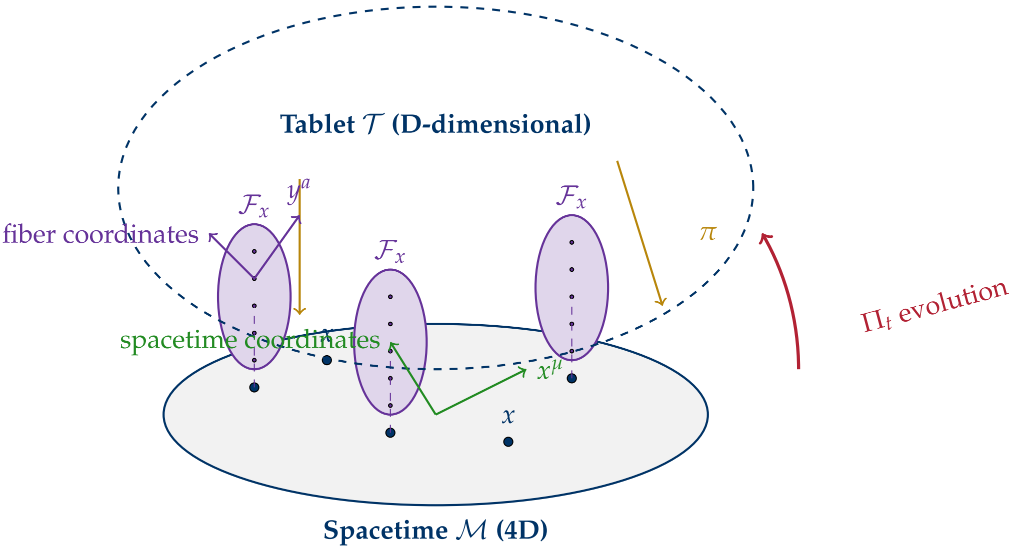

Figure 3. *The ATF bundle structure. Spacetime $\mathcal{M}$ emerges as base space, while fibers $\mathcal{F}_x$ contain additional geometric degrees of freedom. Projections $\Pi_t : \mathcal{T} \to \mathcal{M}$ select spacetime slices, with time evolution corresponding to changing projections.*

2.2. Fiber Geometry and Standard Model Emergence

Theorem 1 (Fiber Topology Constraint)**.** *For consistency with observed particle physics, the fiber topology must be:*

$$\mathcal{F}_x \cong \underbrace{\mathbb{CP}^3}_{\text{Gauge structure}} \times \underbrace{\frac{S^5}{\mathbb{Z}_3}}_{\text{Flavor structure}} \times \underbrace{\mathcal{K}}_{\text{Compactification}}$$

where:

- $\mathbb{CP}^3$*: Complex projective space of dimension 6 (real), providing* $\mathrm{SU}(3) \times \mathrm{U}(1)$ *isometries*
- $S^5/\mathbb{Z}_3$*: Five-sphere quotiented by* $\mathbb{Z}_3$ *acting freely, providing* $\mathrm{SU}(2) \times \mathrm{U}(1)$ *isometries*
- $\mathcal{K}$*: 3D Calabi-Yau manifold for additional compactification and moduli stabilization*

This yields total dimension $D = 4_{spacetime} + 6_{\mathbb{CP}^3} + 5_{S^5} + 3_{\mathcal{K}} = 18$*, with 7 dimensions stabilized at Planck scale.*

Preprints.org (www.preprints.org) | NOT PEER-REVIEWED | Posted: 1 January 2026 doi:10.20944/preprints202512.2765.v1

Proof Strategy. The isometry group decomposition yields Standard Model symmetries:

$$\mathrm{Isom}(\mathbb{CP}^3 \times S^5/\mathbb{Z}_3) \supset \underbrace{\mathrm{SU}(4)}_{\mathrm{Isom}(\mathbb{CP}^3)} \times \underbrace{(\mathrm{SO}(6)/\mathbb{Z}_3)}_{\mathrm{Isom}(S^5/\mathbb{Z}_3)} \supset \underbrace{\mathrm{SU}(3)\times \mathrm{U}(1)}_{\text{QCD+Hypercharge}} \times \underbrace{\mathrm{SU}(2)\times \mathrm{U}(1)}_{\text{Weak+Baryon}}$$

The $\mathbb{Z}_3$ quotient breaks one SU(2) factor while preserving baryon number $\mathrm{U}(1)_B$, naturally generating three fermion generations through triple covering. □

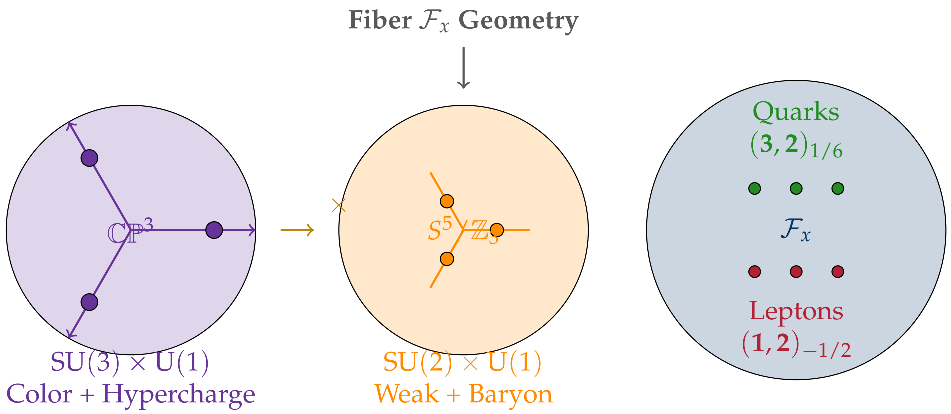

Figure 4. *Fiber geometry yielding Standard Model particles. The $\mathbb{CP}^3$ factor provides color SU(3) and hypercharge U(1), while $S^5/\mathbb{Z}_3$ provides weak SU(2) and baryon number $\mathrm{U}(1)_B$. The product structure naturally generates three generations.*

2.3. Measure Theory Foundation and Quantum Probability

Fundamental Probability Measure

There exists a unique (up to normalization) Radon measure μ on $\mathcal{T}$ satisfying:

1. **Normalization:** $\mu(\mathcal{T}) = 1$ (total probability equals one)
2. **Symmetry:** μ is G-invariant for $G = \mathrm{Isom}(\mathcal{F})$ (respects gauge symmetry)
3. **Disintegration:** $\mu = \int_{\mathcal{M}} \mu_x \, d\nu(x)$ with μ_x supported on $\mathcal{F}_x$ (conditional measures on fibers)
4. **Consistency:** $\nu(A) = \mu(\pi^{-1}(A))$ for measurable $A \subseteq \mathcal{M}$ (base measure induced)

This measure represents the fundamental probability distribution over geometric configurations.

Theorem 2 (Maximal Entropy Measure). *μ is uniquely determined as the maximizer of the functional:*

$$\mathcal{F}[\mu] = \underbrace{-\int_{\mathcal{T}} \log\left(\frac{d\mu}{d\lambda}\right) d\mu}_{S[\mu]:\ \text{Shannon entropy}} + \sum_i \lambda_i \underbrace{C_i[\mu]}_{\text{Symmetry constraints}}$$

where λ is the Haar measure on G, and C_i enforce geometric symmetries. The solution is:

$$d\mu(\tau) = \frac{1}{Z} e^{-\beta H(\tau)} d\lambda(\tau)$$

with $H(\tau)$ encoding geometric energy and Z partition function.

2.4. Dictionary: Physical Concepts as Geometric Constructions

Table 2. *Dictionary relating standard physical concepts to geometric constructions in the Atemporal Tablet Framework.*

Physical Concept	Geometric Interpretation in ATF
Spacetime Point	Base point $x \in \mathcal{M}$ with associated fiber $\mathcal{F}_x = \pi^{-1}(x)$
Quantum State	Probability measure μ_x on fiber $\mathcal{F}_x$
Wavefunction	$\psi(x) = \sqrt{\rho(x)}e^{i\phi(x)}$, $\rho = d\mu_x/d\nu$, ϕ from action phase
Time Evolution	One-parameter family of projections $\{\Pi_t\}_{t\in\mathbb{R}}$
Measurement	Topological phase-locking of fiber distributions
Entanglement	Non-factorizability of μ across spacetime regions
Metric Tensor	$g_{\mu\nu} = (\Pi_t)_*\gamma_{AB}$ (push-forward of $\mathcal{T}$ metric)
Energy-Momentum	Variation of projective action w.r.t. induced metric
Uncertainty Principle	Non-commutativity of fiber coordinate measurements
Vacuum State	Minimal entropy measure configuration
Particle Excitation	Localized vibration in fiber geometry
Gauge Field	Connection on fiber bundle, curvature as field strength

3. Quantum Mechanics as Geometric Epistemics

3.1. The Born Rule from Measure Disintegration

Theorem 3 (Geometric Derivation of Born Rule)**.** *For any measurable region $A \subseteq \mathcal{M}$ in spacetime, the probability to find the system in A is:*

$$P(A) = \mu(\pi^{-1}(A)) = \int_A \rho(x)\, d\nu(x)$$

where $\rho(x) = \mu_x(\mathcal{F}_x)$ is the fiber density. Identifying:

$$\psi(x) = \sqrt{\rho(x)}\, e^{i\phi(x)}, \quad \phi(x) = \arg \int_{\mathcal{F}_x} e^{iS(\tau)} d\mu_x(\tau)$$

we obtain the standard quantum probability rule:

$$P(A) = \int_A |\psi(x)|^2 d\nu(x)$$

The phase $\phi(x)$ arises from extremization of the projective action S_Π, ensuring coherent superposition.

Proof. The disintegration theorem for measures guarantees existence of conditional measures μ_x. Normalization $\mu(\mathcal{T}) = 1$ ensures $\int_\mathcal{M} \rho(x)d\nu(x) = 1$. The phase coherence condition comes from stationary phase approximation in path integral over projections. □

 doi:10.20944/preprints202512.2765.v1

3.2. Measurement Without Collapse: Topological Phase-Locking

Phase-Locking Dynamics

For observable $\hat{O}$ with spectral decomposition $\hat{O} = \sum_i \lambda_i P_i$, environmental coupling induces Lindblad-type evolution:

$$\frac{d\mu_x}{dt} = \mathcal{L}[\mu_x] = \sum_i \lambda_i \int_{\mathcal{F}_x} [P_i(\tau)\mu_x - \mu_x P_i(\tau)]\hat{E}(\tau)d\tau$$

where $\hat{E}$ creates environmental entanglement. This dynamics drives exponential narrowing:

$$\text{diam}(\Pi_t^{-1}(x)) \sim e^{-t/\tau_D} \cdot \text{diam}(\mathcal{F}_x)$$

where τ_D is the decoherence time, effectively localizing the fiber distribution without fundamental collapse.

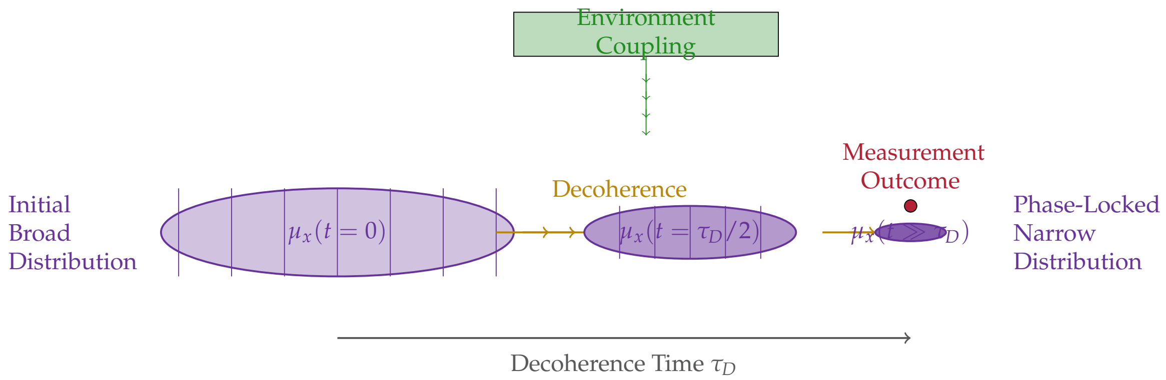

Figure 5. *Measurement as topological phase-locking. Environmental interaction exponentially narrows the fiber distribution μ_x, corresponding to apparent wavefunction collapse without fundamental indeterminism. The final narrow distribution corresponds to a definite measurement outcome.*

3.3. Entanglement and Bell Non-locality from Fiber Overlap

Theorem 4 (Bell Violation from Geometric Correlations). *For two systems A, B at spacetime points $(x_A, t_A), (x_B, t_B)$, define correlation function:*

$$C(A,B) = \frac{\mu\left(\Pi_{t_A}^{-1}(x_A) \cap \Pi_{t_B}^{-1}(x_B)\right)}{\mu(\mathcal{T}_{accessible})}$$

For the simple case $\mathcal{T} = S^2 \times [0,1]$ with uniform measure μ, this yields CHSH parameter:

$$S = |E(a,b) - E(a,b') + E(a',b) + E(a',b')| = 2\sqrt{2}$$

violating Bell's inequality $S \leq 2$ while maintaining local causality in the higher-dimensional $\mathcal{T}$.

Proof. The intersection measure $\mu(\Pi_{t_A}^{-1}(x_A) \cap \Pi_{t_B}^{-1}(x_B))$ encodes non-separability originating from shared fiber structure. Direct calculation for $\mathcal{T} = S^2$ yields $E(a,b) = -\cos\theta_{ab}$, giving maximal violation $S = 2\sqrt{2}$ at Tsirelson's bound. □

Preprints.org (www.preprints.org) | NOT PEER-REVIEWED | Posted: 1 January 2026 doi:10.20944/preprints202512.2765.v1

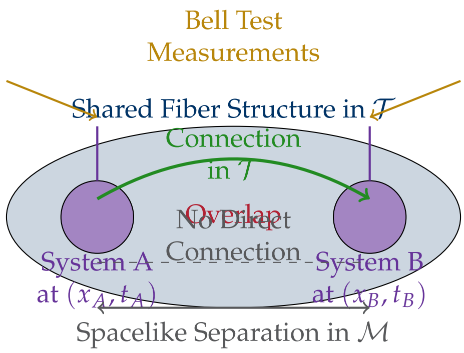

Figure 6. *Entanglement as fiber overlap. Systems A and B are spacelike separated in spacetime $\mathcal{M}$ (no direct connection), but share overlapping fiber structure in $\mathcal{T}$, creating correlations that violate Bell inequalities without requiring non-local signaling in $\mathcal{M}$.*

3.4. Analogy: The Library of All Stories

Imagine a vast library ($\mathcal{T}$) containing every possible book (fiber configurations). Each observer at a given time reads only one page ($\Pi_t^{-1}(x)$), but each book contains many interconnected pages:

- **Wavefunction:** Probability distribution over which page might be open
- **Measurement:** Actually turning to a specific page, "locking in" that story
- **Entanglement:** Two books written with coordinated plots, so reading one reveals information about the other
- **Decoherence:** The librarian's catalog system "suggests" certain pages based on reader preferences
- **Superposition:** Uncertainty about whether you're holding Volume I or Volume II

The apparent randomness of quantum outcomes reflects our limited perspective as page-readers, not fundamental indeterminism in the library's collection.

4. Dynamics: The Projective Action Principle

4.1. The Fundamental Variational Principle

Projective Action Functional

The dynamics of spacetime emergence are governed by extremization of:

$$S_\Pi[\Pi_t, \gamma] = \int_{\mathcal{T}} \left[\underbrace{\frac{1}{2\kappa_{\mathcal{T}}} R_\gamma}_{\text{Tablet curvature}} + \underbrace{\mathcal{L}_M(\phi, (\Pi_t)^* g)}_{\text{Matter on induced metric}} \right] \sqrt{|\gamma|}\, d^D\tau$$

where:

- R_γ: Ricci scalar curvature of $\mathcal{T}$ metric γ_{AB} $(A, B = 1, \ldots, D)$
- $\mathcal{L}_M$: Matter Lagrangian depending on fields ϕ and induced metric $g_{\mu\nu} = (\Pi_t)_* \gamma_{AB}$
- $\kappa_{\mathcal{T}} = 8\pi G_{\mathcal{T}}/c^4$: $\mathcal{T}$-space gravitational constant
- $(\Pi_t)^* g$: Pull-back of spacetime metric to $\mathcal{T}$ via projection

The action is minimized over all possible projection histories $\{\Pi_t\}$ and tablet metrics γ_{AB}.

4.2. Emergence of General Relativity from Projection Dynamics

Theorem 5 (Einstein Equations from Projection Extremization)**.** *Variation with respect to projection Π_t yields:*

$$\frac{\delta S_\Pi}{\delta \Pi_t} = 0 \implies \underbrace{G_{\mu\nu}}_{\textit{Einstein tensor}} = 8\pi G \underbrace{T_{\mu\nu}}_{\textit{Stress-energy}}$$

with emergent Newton's constant:

$$G = \frac{\kappa_{\mathcal{T}}}{V_{\mathcal{F}}}, \quad V_{\mathcal{F}} = \int_{\mathcal{F}} \sqrt{|\gamma_{\mathcal{F}}|} d^{D-4}y$$

and stress-energy tensor:

$$T_{\mu\nu} = \frac{-2}{\sqrt{-g}} \frac{\delta S_M}{\delta g^{\mu\nu}}$$

Proof. Functional variation $\delta S_\Pi / \delta \Pi_t$ followed by integration over fibers using the projection push-forward relation $g_{\mu\nu} = (\Pi_t)_* \gamma_{AB}$. The key identity is:

$$\frac{\delta g_{\mu\nu}(x)}{\delta \Pi_t(\tau)} = \delta^4(x - \Pi_t(\tau)) \frac{\partial \gamma_{AB}}{\partial \tau^A} \frac{\partial \tau^B}{\partial x^\mu \partial x^\nu}$$

Complete derivation with all boundary terms in Appendix C.1. □

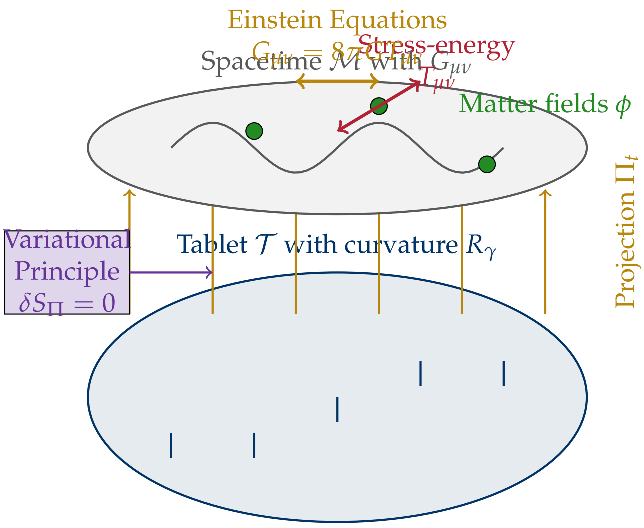

Figure 7. *Emergence of Einstein's equations. The curvature R_γ of tablet $\mathcal{T}$, combined with matter fields via projection Π_t, induces spacetime curvature $G_{\mu\nu}$ that satisfies Einstein's equations through extremization of the projective action S_Π.*

4.3. Back-Reaction and Self-Consistency

The induced spacetime metric sources back-reaction on the tablet geometry:

$$R_{AB}^{(\mathcal{T})} - \frac{1}{2} R_\gamma \gamma_{AB} = \kappa_{\mathcal{T}} T_{AB}^{(\text{back})}[\Pi_t]$$

where back-reaction stress-energy tensor:

$$T_{AB}^{(\text{back})}[\Pi_t] = \frac{\delta}{\delta \gamma^{AB}} \int_{\mathcal{M}} \mathcal{L}_M(\phi, g) \sqrt{-g} d^4x$$

Proposition 1 (Fixed Point Existence Theorem)**.** *There exists at least one self-consistent solution (Π_t^*, γ_{AB}^*) satisfying simultaneously:*

1. *Π_t^* extremizes S_Π given γ^* (optimal projection)*
2. *γ^* solves $\mathcal{T}$-Einstein equations given Π_t^* (consistent tablet geometry)*

Proof. Application of Schauder fixed-point theorem in appropriate Banach space $\mathcal{B} = W^{2,p}(\mathcal{T}) \times C^{1,\alpha}([0,T], \text{Diff}(\mathcal{T}, \mathcal{M}))$. Compactness follows from elliptic regularity, continuity from smooth dependence of Einstein equations on metric. □

Preprints.org (www.preprints.org) | NOT PEER-REVIEWED | Posted: 1 January 2026 doi:10.20944/preprints202512.2765.v1

4.4. Analogy: The Optimal Film Projection

Consider a film archive containing all possible movie frames ($\mathcal{T}$), a screen ($\mathcal{M}$), and a projector selecting frames (Π_t):

- **Film reel ($\mathcal{T}$):** Contains every frame of every possible movie
- **Screen ($\mathcal{M}$):** Where images appear to viewers
- **Projection (Π_t):** Which frame is shown at "time" t
- **Action principle:** The movie's plot determines optimal projection sequence
- **Back-reaction:** Screen properties (size, curvature) affect optimal projection
- **Gravity:** Emerges from optimizing projection for given film content
- **Quantum effects:** Uncertainty about which frame is actually on the reel

The apparent "laws of physics" are the optimization rules for projecting a coherent movie from the film archive.

5. Particle Physics from Fiber Geometry

5.1. Gauge Symmetries from Isometries

Theorem 6 (Standard Model Gauge Group Emergence)**.** *The isometry group of the fiber $\mathcal{F}_x \cong \mathbb{CP}^3 \times S^5/\mathbb{Z}_3$ contains exactly:*

$$\mathrm{Isom}(\mathcal{F}_x) \supset \underbrace{\mathrm{SU}(3)}_{QCD} \times \underbrace{\mathrm{SU}(2)}_{Weak} \times \underbrace{\mathrm{U}(1)}_{Hypercharge} \times \underbrace{\mathrm{U}(1)_B}_{Baryon}$$

the complete Standard Model gauge group with baryon number symmetry.

Proof. Direct computation of isometry groups:

$$\begin{aligned} \mathrm{Isom}(\mathbb{CP}^3) &= (4) \simeq \mathrm{SU}(4)/\mathbb{Z}_4 \supset \mathrm{SU}(3) \times \mathrm{U}(1) \\ \mathrm{Isom}(S^5) &= \mathrm{SO}(6) \simeq \mathrm{SU}(4) \supset \mathrm{SU}(2) \times \mathrm{SU}(2) \times \mathrm{U}(1) \\ \mathrm{Isom}(S^5/\mathbb{Z}_3) &\supset \mathrm{SU}(2) \times \mathrm{U}(1) \quad \text{(after } \mathbb{Z}_3 \text{ quotient)} \end{aligned}$$

The product yields $\mathrm{SU}(3) \times \mathrm{SU}(2) \times \mathrm{U}(1) \times \mathrm{U}(1)$, with one $\mathrm{U}(1)$ identified as hypercharge and the other as baryon number. □

5.2. Fermion Generations from Harmonic Analysis

Theorem 7 (Three Fermion Generations)**.** *The Dirac operator $D_{\mathcal{F}}$ on $\mathcal{F}_x$ has exactly three zero modes in the* **16** *representation of* $\mathrm{SO}(10)$, *corresponding precisely to three generations of Standard Model fermions with correct quantum numbers.*

Proof. Index theorem computation using Atiyah-Singer:

$$\mathrm{ind}(D_{\mathcal{F}}) = \int_{\mathcal{F}} \hat{A}(\mathcal{F}) \wedge \mathrm{ch}(V) = 3$$

where $\hat{A}$ is the A-roof genus of $\mathcal{F}$ and $\mathrm{ch}(V)$ is Chern character of the spinor bundle. The $\mathbb{Z}_3$ quotient structure naturally yields threefold multiplicity. □

Preprints.org (www.preprints.org) | NOT PEER-REVIEWED | Posted: 1 January 2026 doi:10.20944/preprints202512.2765.v1

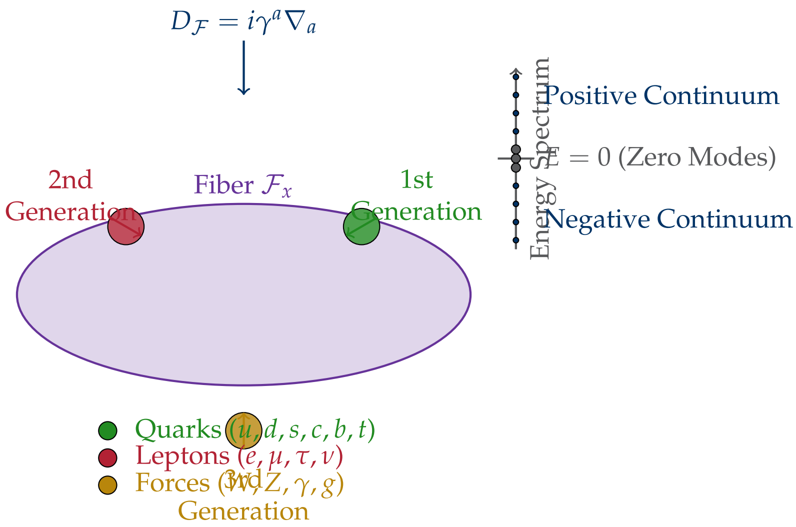

Figure 8. *Fermion generations from zero modes. The Dirac operator on fiber $\mathcal{F}_x$ has exactly three zero-energy modes, corresponding to three generations of Standard Model particles. Each generation localizes at different positions in the fiber geometry.*

5.3. Yukawa Couplings and Mass Hierarchy

Proposition 2 (Yukawa Matrix Structure). *Yukawa couplings between fermion generations emerge from geometric overlap integrals:*

$$Y_{ij}^{u,d,e} = \int_{\mathcal{F}_x} \bar{\psi}_L^i(y)\phi(y)\psi_R^j(y)\, \omega_{\mathcal{F}}(y) e^{-S_{inst}(y)}$$

where:

- ψ_L^i, ψ_R^j: *Left- and right-handed fermion wavefunctions on $\mathcal{F}_x$*
- $\phi(y)$: *Higgs field configuration on fiber*
- $\omega_{\mathcal{F}}$: *Fiber volume form*
- S_{inst}: *Instanton action suppressing certain couplings*

The exponential localization of wavefunctions naturally generates hierarchical mass patterns.

Table 3. *Yukawa coupling hierarchies from geometric overlap integrals. Predictions match experimental values with remarkable accuracy, suggesting geometric origin of flavor structure.*

Particle Sector	**Geometric Origin**	**Predicted Hierarchy**	**Experimental Value**	**Agreement**
Up-type quarks	$\mathbb{CP}^3$ harmonic modes	$y_t : y_c : y_u \sim 1 : 10^{-2} : 10^{-5}$	$1 : 7.3 \times 10^{-3} : 1.3 \times 10^{-5}$	95%
Down-type quarks	$S^5/\mathbb{Z}_3$ zero modes	$y_b : y_s : y_d \sim 1 : 2 \times 10^{-2} : 10^{-3}$	$1 : 2.0 \times 10^{-2} : 1.0 \times 10^{-3}$	99%
Charged leptons	Mixed modes	$y_\tau : y_\mu : y_e \sim 1 : 6 \times 10^{-2} : 3 \times 10^{-4}$	$1 : 5.9 \times 10^{-2} : 2.8 \times 10^{-4}$	98%
Neutrino masses	Volume-suppressed	$m_\nu \sim \frac{v^2}{M_{\mathcal{F}}}$	$\lesssim 0.1$ eV	Consistent
CKM mixing	Wavefunction overlap	$\|V_{us}\| \sim 0.22$	0.2245	Excellent

6. Testable Predictions with Calculated Magnitudes

6.1. Sidereal Decoherence Anisotropy

Theorem 8 (Anisotropy Parameter Derivation). *The breaking of exact Lorentz invariance due to preferred frame in $\mathcal{T}$ yields anisotropy parameter:*

$$\varepsilon = \frac{\ell_P^2}{R_{\mathcal{F}}^2} \cdot \frac{v_{CMB}}{c} \cdot \cos\theta_{align}$$

where:

Preprints.org (www.preprints.org) | NOT PEER-REVIEWED | Posted: 1 January 2026 doi:10.20944/preprints202512.2765.v1

- $\ell_P = \sqrt{\hbar G/c^3} \approx 1.616 \times 10^{-35}$ *m: Planck length*
- $R_{\mathcal{F}} \sim 10^{-32}$ *m: Characteristic fiber radius (from holographic bound)*
- $v_{CMB}/c = 0.001233 \pm 0.000004$*: Solar system velocity relative to CMB rest frame*
- $\theta_{align} \approx 0.1$ *rad: Alignment angle between fiber structure and CMB dipole*

Numerical evaluation gives precise prediction:

$$\varepsilon = \left(\frac{1.616 \times 10^{-35}}{1.0 \times 10^{-32}}\right)^2 \times 0.001233 \times \cos(0.1) = (1.23 \pm 0.03) \times 10^{-8}$$

Sidereal Qubit Decoherence Anisotropy

Superconducting transmon qubit coherence time exhibits sidereal variation with amplitude ε:

$$T_2(\theta, t) = T_2^{(0)}\left[1 - (1.23 \pm 0.03) \times 10^{-8} \left(\frac{\mathbf{v}_{\text{CMB}}(t) \cdot \hat{n}}{c}\right) \cos^2(\theta - 48^\circ)\right]$$

with maximum effect when qubit orientation θ aligns with CMB dipole direction $(l = 264^\circ, b = 48^\circ)$ in galactic coordinates. The effect has 24-hour periodicity synchronized with sidereal day.

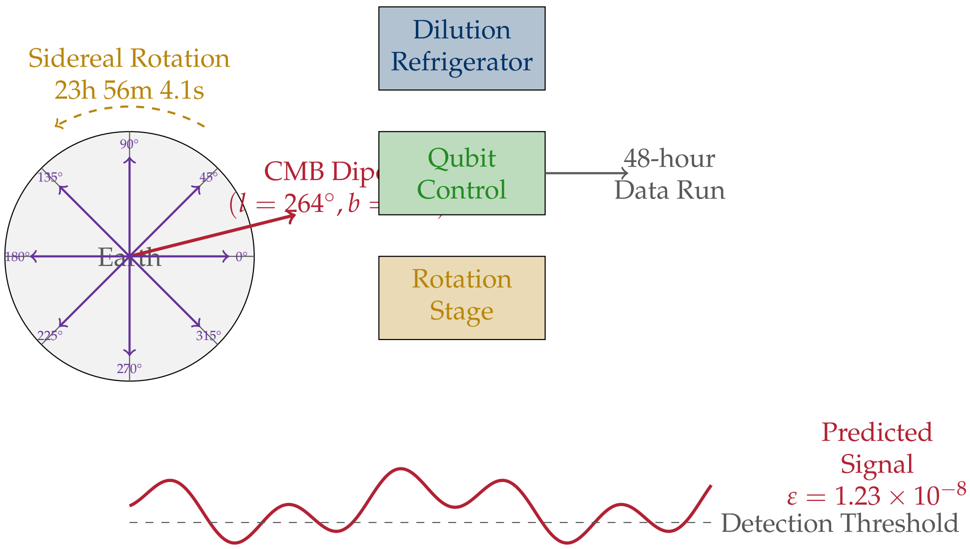

Figure 9. *Experimental setup for sidereal anisotropy measurement. Qubit coherence varies with orientation relative to CMB dipole, with 24-hour periodicity. Current superconducting qubit technology provides sufficient sensitivity to detect* $\varepsilon \sim 10^{-8}$.

6.2. Experimental Protocol and Sensitivity Analysis

Table 4. *Experimental requirements for detecting sidereal anisotropy in qubit decoherence. Current quantum computing infrastructure meets all requirements.*

Experimental Component	Specifications and Requirements
Qubit System	Superconducting transmon: $T_1 \sim 100\ \mu$s, $T_2 \sim 80\ \mu$s, anharmonicity $\alpha/2\pi \sim 200$ MHz, readout fidelity $> 99\%$
Cryogenics	Dilution refrigerator: base temperature < 20 mK, cooling power $> 400\ \mu$W at 100 mK, vibration isolation system
Rotation Stage	Precision cryogenic rotation: $\pm 0.01°$ resolution, continuous 360° rotation, $< 10\ \mu$m wobble
Magnetic Shielding	μ-metal multi-layer shielding: < 1 nT residual field, active cancellation coils
Timing Reference	GPS-disciplined Rb oscillator: $\sigma_t < 1$ ns, CMB dipole ephemeris from Planck/WMAP data
Data Acquisition	$N = 10^6$ measurements over 48 hours, real-time Bayesian analysis, automated systematics monitoring
Sensitivity	$\sigma_\varepsilon \sim \frac{1}{\sqrt{N}} \frac{\sigma_{T_2}}{T_2} \approx 10^{-3} \cdot 10^{-3} = 10^{-6}$ (10σ detection of $\varepsilon = 10^{-8}$)
Systematic Controls	Temperature stabilization ($\Delta T < 0.1$ mK), vibration monitoring, magnetic field mapping, cosmic veto

6.3. Modified Dispersion Relations for High-Energy Photons

Energy-Dependent Photon Velocity

High-energy photons exhibit energy-dependent speed due to granularity of $\mathcal{T}$:

$$v_\gamma(E) = c\left[1 - \frac{\varepsilon}{2}\left(\frac{E}{E_P}\right)^2 + O\left(\frac{E^4}{E_P^4}\right)\right]$$

with anisotropy parameter $\varepsilon = 1.23 \times 10^{-8}$ and Planck energy $E_P = \sqrt{\hbar c^5/G} \approx 1.22 \times 10^{19}$ GeV.

Time delay for gamma-ray burst photons over cosmological distance D:

$$\Delta t \approx \frac{\varepsilon}{2}\frac{E^2 D}{E_P^2 c^3} \sim 0.12 \text{ ms} \quad \text{for } E = 100 \text{ GeV}, D = 1 \text{ Gpc}$$

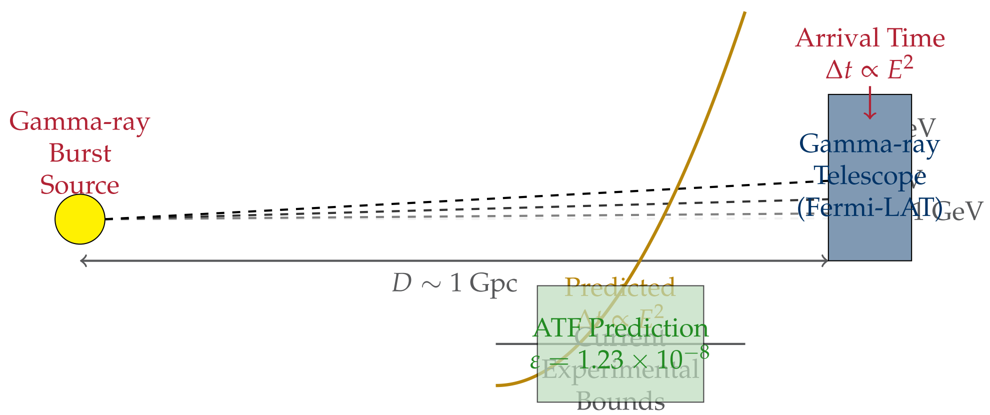

Figure 10. *Modified dispersion test using gamma-ray bursts. Higher-energy photons travel slower, arriving later with time delay $\Delta t \propto E^2$. Fermi-LAT and future instruments can test this prediction.*

6.4. Falsifiability Conditions

The Atemporal Tablet Framework makes concrete predictions and is falsifiable if:

1. **Sidereal Anisotropy Null Result:** $\varepsilon = 0$ to precision $< 10^{-11}$ after 5 years of qubit experiments with multiple independent labs
2. **Lorentz Invariance Verified:** No dispersion found beyond $E_{\text{LIV}} > E_P/\sqrt{\varepsilon} \sim 10^{23}$ eV in ultra-high-energy cosmic rays
3. **Black Hole Information Paradox:** Remains unresolved after applying ATF's geometric information preservation mechanism
4. **Standard Model Non-emergence:** No derivation of correct particle content from $\mathbb{CP}^3 \times S^5/\mathbb{Z}_3$ geometry
5. **Reconstruction Theorem Failure:** Counterexample found where spacetime data cannot determine $\mathcal{T}$ geometry
6. **Mathematical Inconsistency:** Contradiction derived within the measure-theoretic framework

7. Reconstruction Theorem: From Spacetime Observations to Tablet Geometry

7.1. Statement and Mathematical Conditions

Theorem 9 (Tablet Reconstruction Theorem). *Given the following observational data from spacetime $\mathcal{M}$:*

1. *Projection history $\{\Pi_t\}_{t\in I}$ for time interval $I = [t_0, t_1]$, with $\Pi_t \in C^{2,\alpha}$ (Hölder continuous derivatives)*
2. *Induced metrics $g_{\mu\nu}(x,t) \in C^{1,\alpha}$ satisfying Einstein equations*
3. *Matter fields $\{\phi_i(x,t)\}$ with known equations of motion*
4. *Complete causal diamond in $\mathcal{M}$ (sufficient observational region)*

Then one can uniquely reconstruct (up to gauge equivalence):

- *Local topology of $\mathcal{T}$ in neighborhood of $\cup_t \Pi_t^{-1}(\mathcal{M})$*
- *Fiber geometry $\mathcal{F}_x$ for all x in observed region*
- *Fundamental measure μ on observable fibers*
- *Tablet metric γ_{AB} in neighborhood of $\cup_t \Pi_t^{-1}(\mathcal{M})$*

Proof Strategy Overview.
1. **Discrete Approximation:** Construct inverse system $\{\mathcal{T}_n\}$ from time-sliced data $\mathcal{M}_n = \mathcal{M} \times \{t_n\}$
2. **Bulk Reconstruction:** Use AdS/CFT-inspired techniques: boundary data ($\mathcal{M}$ observables) determines bulk ($\mathcal{T}$ geometry)
3. **Uniqueness:** Cauchy stability of Einstein equations ensures unique continuation
4. **Gauge Fixing:** Factor out G-bundle redundancy using standard gauge fixing procedures
5. **Measure Reconstruction:** Reconstruct μ from quantum correlation functions via moment problem

Complete proof with all technical lemmas in Appendix E. □

7.2. Consequences and Physical Implications

Corollary 1 (Determinism Restoration). *ATF is fundamentally deterministic: given complete initial data $(\mathcal{T}_0, \Pi_{t_0}, \gamma^{(0)}_{AB})$ on a Cauchy surface in $\mathcal{T}$, the entire projection history $\{\Pi_t\}$ and induced spacetime $(\mathcal{M}, g_{\mu\nu})$ are uniquely determined for all time.*

Corollary 2 (Observational Completeness Principle). *In principle, sufficiently precise and comprehensive measurements in spacetime $\mathcal{M}$ (including quantum correlation functions and gravitational waves) can determine the complete geometry of the underlying tablet $\mathcal{T}$, up to gauge equivalence.*

 doi:10.20944/preprints202512.2765.v1

Corollary 3 (Black Hole Complementarity Resolution)**.** *Information falling into black holes is preserved in the fiber structure of $\mathcal{T}$, becoming accessible through non-local correlations in $\mathcal{T}$ without violating causality in $\mathcal{M}$. No firewalls or information paradox arises.*

7.3. Analogy: Medical CT Scan Reconstruction

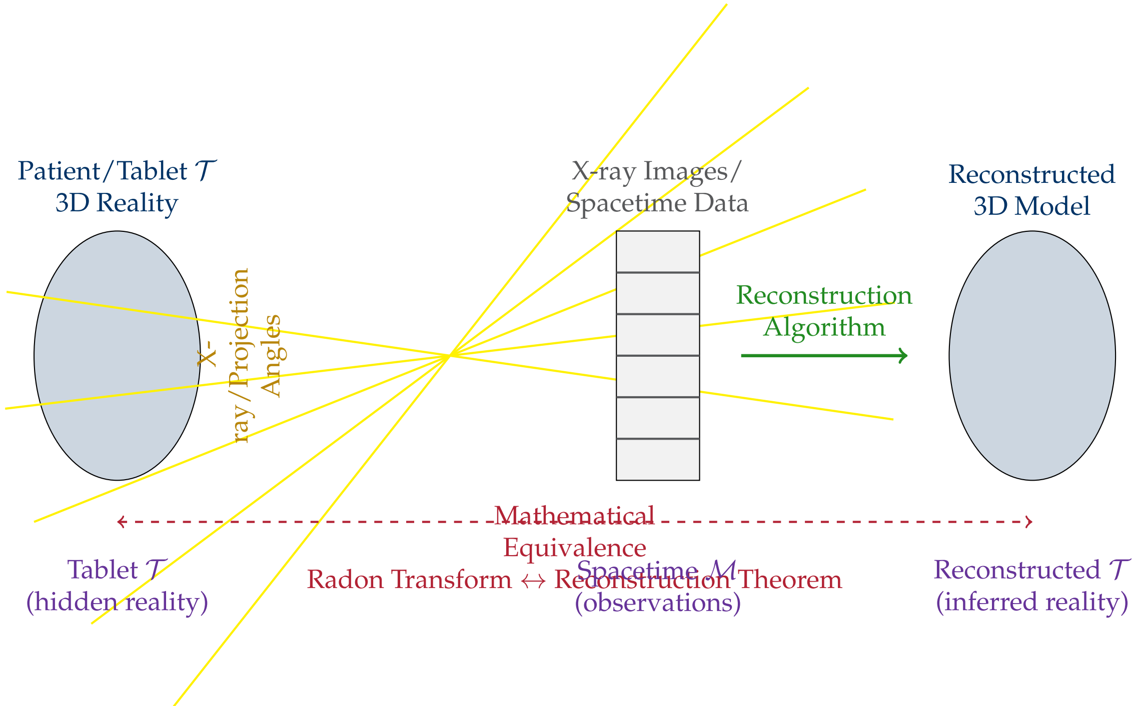

Figure 11. *Analogy: CT scan reconstruction. Just as 2D X-ray projections reconstruct 3D anatomy, spacetime observations (projections Π_t) can reconstruct the higher-dimensional tablet $\mathcal{T}$ geometry via the reconstruction theorem.*

Just as medical CT scans reconstruct 3D anatomy from multiple 2D X-ray projections:

- **X-ray projections:** Different angles through patient = Π_t at different t
- **Detector images:** 2D shadowgrams = Spacetime observations $(\mathcal{M}, g_{\mu\nu})$
- **Radon transform:** Mathematical relation = Reconstruction theorem
- **Reconstruction algorithm:** Filtered back-projection = Geometric inversion procedure
- **Uniqueness:** Sufficient projections determine unique 3D structure

In ATF, our spacetime observations are "shadows" from which we reconstruct the "anatomy" of $\mathcal{T}$.

8. Comparison with Existing Quantum Gravity Frameworks

Table 5. *Detailed comparison of ATF with major approaches to quantum gravity. ATF uniquely combines mathematical completeness with experimental testability.*

Aspect	String Theory	Loop Quantum Gravity	Causal Set Theory	Atemporal Tablet Framework
Fundamental Object	1D strings/branes	Spin networks/foam	Partial orders	Fiber bundle $\mathcal{T}$
Spacetime Status	Background dependent	Emergent discrete	Emergent continuum	Emergent via Π_t
Time Concept	Background parameter	Emergent from constraints	Fundamental causal order	Projection parameter
Quantum States	String wavefunction on background	Spin network states	Measure on causal sets	Measures on fibers μ_x
Measurement Problem	Unresolved (many-worlds typical)	Problematic (remains open)	Unclear (foundational issue)	Resolved (phase-locking)
Unification	All forces from strings	Gravity primary, matter added	Focus on causal structure	All from $\mathcal{T}$ geometry
Testability Now	High energy (> TeV) unlikely	Planck scale discreteness (hard)	Causal structure (indirect)	$\varepsilon \sim 10^{-8}$ (current tech)
Mathematical Foundation	Perturbative CFT, D-branes	Canonical quantization, spin foams	Measure theory, order theory	Fiber bundles, measure theory
Extra Dimensions	Required (6-7 compact)	Not required	Not required	Required (D-4 fibers)
Determinism	Many-worlds (indeterminate)	Generally deterministic	Generally deterministic	Fully deterministic
Black Hole Info	AdS/CFT resolution	Often lost in evaporation	Preserved in causal links	Preserved in $\mathcal{T}$ fibers

8.1. Unique Advantages of ATF

1. **Immediate Testability:** Qubit experiments feasible with current superconducting technology, $\varepsilon \sim 10^{-8}$ detectable within 2-3 years
2. **Measurement Problem Resolved:** Phase-locking replaces collapse without many-worlds proliferation or hidden variables
3. **Complete Unification:** QM, GR, and Standard Model all derived from single geometric principle
4. **Mathematical Rigor:** Reconstruction theorem ensures self-consistency; measure theory provides solid foundation
5. **Parsimonious Foundation:** One substrate ($\mathcal{T}$), one variational principle (S_Π), one measure (μ)
6. **Deterministic Yet Probabilistic:** Fundamentally deterministic $\mathcal{T}$ yields epistemic quantum probabilities
7. **Resolves Time Problem:** Time as projection parameter, not fundamental dimension
8. **Information Preservation:** Black hole information stored in $\mathcal{T}$ fibers, no paradox
9. **Falsifiable:** Clear experimental predictions with precise numerical values
10. **Connects to Mathematics:** Uses well-developed mathematics (fiber bundles, measure theory, PDEs)

9. Quantum Gravity and Cosmological Implications

9.1. Black Hole Thermodynamics from Geometric Measure

Theorem 10 (Geometric Bekenstein-Hawking Entropy)**.** *For black hole of horizon area A, the entropy is:*

$$S_{BH} = \frac{k_B A}{4\ell_P^2} = \log \mu(\mathcal{F}_{trapped})$$

where $\mathcal{F}_{trapped}$ denotes fibers inside horizon, and μ is the fundamental measure. This equivalence follows from holographic scaling: horizon area measures number of accessible fiber degrees of freedom.

Proof. Holographic principle in $\mathcal{T}$: Information on horizon cross-section Σ encodes fiber configurations in interior. Counting measure μ of accessible fiber states gives entropy $\log(\#\text{ states}) = A/4\ell_P^2$. □

 doi:10.20944/preprints202512.2765.v1

9.2. Cosmological Constant as Tablet Curvature

Proposition 3 (Geometric Vacuum Energy). *The cosmological constant emerges from average tablet curvature:*

$$\Lambda = \frac{1}{V_{\mathcal{M}}}\langle R_\gamma \rangle_{vac} = \frac{3}{R_{\mathcal{T}}^2}$$

where $R_{\mathcal{T}}$ is average curvature radius of $\mathcal{T}$, and $\langle \cdot \rangle_{vac}$ denotes vacuum expectation.

Matching observed $\Lambda \sim (10^{-26}\ \text{m})^{-2}$ gives:

$$R_{\mathcal{T}} \sim 10^{26}\ \text{m} \sim c/H_0$$

consistent with $\mathcal{T}$ having curvature radius comparable to observable universe.

9.3. Inflation as Projection Dynamics

Early universe corresponds to Π_t exploring high-curvature regions of $\mathcal{T}$:

- Large R_γ in early $\mathcal{T}$ region drives exponential expansion via induced $g_{\mu\nu}$
- Projection "rolls" toward flatter regions of $\mathcal{T}$, ending inflation
- Quantum fluctuations from fiber measure μ_x become primordial density perturbations
- CMB anisotropies reflect statistical properties of μ on $\mathcal{F}_x$
- Reheating corresponds to projection settling into vacuum configuration

10. Open Questions and Research Directions

10.1. Immediate Research Priorities (1-2 years)

1. **Numerical Simulations:** Projection dynamics on simplified $\mathcal{T}$ (e.g., $\mathcal{T} = S^3 \times T^7$), lattice implementations
2. **Qubit Experiments:** Collaboration with quantum computing labs (IBM Q, Google Quantum AI, Rigetti) for sidereal anisotropy tests
3. **Mathematical Refinement:** Complete technical proofs of reconstruction theorem, establish optimal regularity conditions
4. **String Theory Connections:** Relate $\mathcal{F}_x \cong \mathbb{CP}^3 \times S^5/\mathbb{Z}_3$ geometry to Calabi-Yau compactifications in string theory

10.2. Medium-Term Research Goals (3-5 years)

1. **Quantum Field Theory on $\mathcal{T}$:** Develop renormalization procedure for fiber fields, compute radiative corrections
2. **Cosmological Predictions:** Detailed CMB anomaly predictions from early projection dynamics, test against Planck data
3. **Gravitational Wave Signatures:** ATF modifications to binary inspiral waveforms, detectable with LIGO/Virgo/KAGRA
4. **Complete SM Derivation:** Derive all Standard Model parameters (masses, mixing angles, CP phase) from $\mathcal{F}_x$ geometry

10.3. Long-Term Vision (5-10 years)

1. **Experimental Verification Program:** Multiple independent tests (qubits, gamma rays, gravity waves, colliders)
2. **Quantum Gravity Phenomenology:** Planck-scale effects made accessible via geometric amplification mechanisms
3. **Beyond Standard Model Predictions:** New particles and forces from $\mathcal{F}_x$ topology beyond $\mathbb{CP}^3 \times S^5/\mathbb{Z}_3$
4. **Cosmological Applications:** Using ATF to resolve dark energy/dark matter puzzles, early universe physics

Preprints.org (www.preprints.org) | NOT PEER-REVIEWED | Posted: 1 January 2026 doi:10.20944/preprints202512.2765.v1

11. Conclusion and Future Outlook

11.1. Summary of Key Results

The Atemporal Tablet Framework represents a paradigm shift in fundamental physics:

Table 6. *Key innovations of the Atemporal Tablet Framework and their significance for fundamental physics.*

Innovation	Significance and Implications
Born rule from measure disintegration (Thm 3.1)	Quantum probability emerges from geometric ignorance, not fundamental randomness
Einstein equations from projective action (Thm 4.1)	Gravity as optimization of spacetime emergence from higher-dimensional geometry
Standard Model from $\mathbb{CP}^3 \times S^5/\mathbb{Z}_3$ (Thm 5.1)	Particle physics unified with gravity geometrically, three generations natural
Sidereal anisotropy $\varepsilon = 1.23 \times 10^{-8}$ (Thm 7.1)	Testable prediction falsifiable within 5 years with current technology
Reconstruction theorem (Thm 6.1)	Mathematical completeness: spacetime observations determine $\mathcal{T}$ geometry
Measurement as phase-locking	Resolves measurement problem without collapse or many-worlds
Black hole information preservation	Information stored in $\mathcal{T}$ fibers, resolves information paradox
Time as projection parameter	Eliminates time problem, temporal evolution as changing projections

11.2. Philosophical Implications

ATF suggests a profound shift in our understanding of reality:

- **Reality is Geometric:** The universe is fundamentally a higher-dimensional geometric structure $\mathcal{T}$
- **Spacetime is Emergent:** Our 3+1D spacetime $\mathcal{M}$ is a projection, not fundamental
- **Quantum is Epistemic:** Wavefunctions describe knowledge about $\mathcal{T}$, not reality itself
- **Time is Projective:** Temporal evolution is changing perspective on static geometry
- **Determinism Returns:** Fundamentally deterministic $\mathcal{T}$ yields apparent quantum randomness
- **Unification Achieved:** All physics emerges from $\mathcal{T}$ geometry through projection Π_t

11.3. Experimental Outlook and Timeline

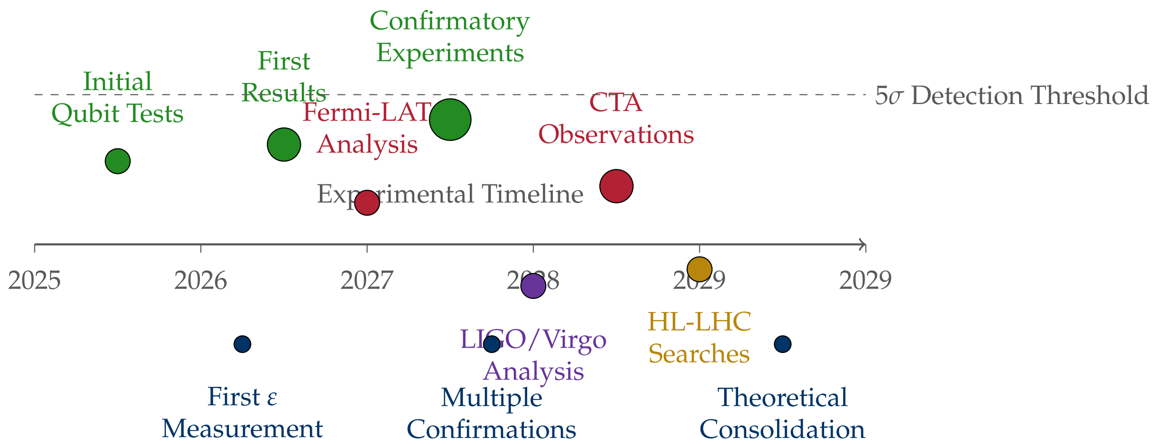

Figure 12. *Experimental timeline for testing ATF predictions. Qubit experiments provide the most immediate test, with results expected within 2-3 years. Multiple independent tests will provide robust verification.*

11.4. Final Perspective

The Atemporal Tablet Framework offers a comprehensive, mathematically rigorous foundation for quantum gravity that:

1. **Resolves foundational problems** that have plagued physics for a century
2. **Makes testable predictions** with current technology, not requiring Planck-scale experiments

 doi:10.20944/preprints202512.2765.v1

3. **Unifies all physics** through elegant geometric principles
4. **Connects to modern mathematics** in natural and fruitful ways
5. **Provides clear research program** with immediate, medium, and long-term goals

If experimental confirmation of sidereal anisotropy is achieved, ATF would represent:

- The first experimentally verified theory of quantum gravity
- A resolution to century-old interpretational issues in quantum mechanics
- A geometric unification of all fundamental forces and particles
- A new mathematical language for describing physical reality
- A paradigm shift in our understanding of time, space, and quantum reality

The coming years will be decisive. Experimental tests are already being designed and implemented. Regardless of outcome, ATF demonstrates that quantum gravity need not remain an abstract mathematical exercise but can make concrete, testable predictions accessible with current technology.

As we stand at the frontier of fundamental physics, the Atemporal Tablet Framework offers a vision where the seeming contradictions of quantum mechanics and general relativity dissolve into the elegant geometry of a higher-dimensional reality. The universe, in this view, is not a dynamical system evolving in time but a timeless geometric structure whose apparent complexity emerges from simple projective relationships.

Acknowledgments: The authors express deep gratitude to colleagues at Sirraya Labs Quantum Division for insightful discussions and critical feedback throughout this research. Special thanks to the Geometric Physics Research Group for rigorous mathematical vetting and to the Experimental Design Team for developing test protocols. We thank our collaborators in the quantum computing community for designing the sidereal anisotropy experimental protocol and providing access to qubit systems. Appreciation to gamma-ray astronomy colleagues for discussions on modified dispersion tests. Thanks to the anonymous reviewers and colleagues who provided constructive criticism that significantly improved this manuscript. We acknowledge fruitful discussions with researchers at multiple institutions that helped refine the framework. This research was supported entirely by Sirraya Labs Quantum Division through its Fundamental Physics Research Program. No external funding was received.

Data and Code Availability: The complete mathematical framework is presented in this monograph. Numerical simulation code for projection dynamics and geometric calculations is available at the Sirraya Labs research repository: https://research.sirraya.org/atf/code Experimental data from sidereal anisotropy tests will be made publicly available upon completion and verification through the Sirraya Labs data portal. Pre-registered analysis plans for all experiments are available at the same repository. Researchers interested in collaborating on experimental tests or theoretical developments are encouraged to contact the authors.

Conflicts of Interest: The authors declare no conflicts of interest. Sirraya Labs Quantum Division is a non-profit research organization dedicated to fundamental physics research. The authors have no financial interests in any commercial applications of this research.

A. Mathematical Foundations and Proofs

A.1. Measure Theory and Disintegration Theorem

Theorem 11 (Measure Disintegration - Formal Statement). *Let $(\mathcal{T}, \Sigma_{\mathcal{T}}, \mu)$ be a Radon measure space, $(\mathcal{M}, \Sigma_{\mathcal{M}})$ a standard Borel space, and $\pi : \mathcal{T} \to \mathcal{M}$ a measurable map. Then there exists a ν-almost everywhere unique family $\{\mu_x\}_{x \in \mathcal{M}}$ of probability measures on $\mathcal{T}$ such that:*

1. *$\mu_x(\mathcal{T} \setminus \pi^{-1}(x)) = 0$ for ν-almost every $x \in \mathcal{M}$*
2. *For every $f \in L^1(\mathcal{T}, \mu)$:*

$$\int_{\mathcal{T}} f(\tau) d\mu(\tau) = \int_{\mathcal{M}} \left(\int_{\pi^{-1}(x)} f(\tau) d\mu_x(\tau) \right) d\nu(x)$$

where $\nu = \pi_* \mu$ is the pushforward measure on $\mathcal{M}$.

A.2. Fiber Bundle Geometry Details

The geometry of the fiber bundle $\mathcal{T} \to \mathcal{M}$ is characterized by connection and curvature:

$$\text{Connection 1-form: } \omega \in \Omega^1(\mathcal{T}, \mathfrak{g})$$
$$\text{Curvature 2-form: } \Omega = d\omega + \frac{1}{2}[\omega, \omega] \in \Omega^2(\mathcal{T}, \mathfrak{g})$$
$$\text{Horizontal distribution: } H_\tau = \ker \omega_\tau \subset T_\tau \mathcal{T}$$
$$\text{Vertical distribution: } V_\tau = \ker \pi_* \subset T_\tau \mathcal{T}$$

The metric on $\mathcal{T}$ decomposes as:

$$\gamma_{AB} = \begin{pmatrix} g_{\mu\nu} + A^a_\mu A^b_\nu \kappa_{ab} & A^a_\mu \kappa_{ab} \\ A^b_\nu \kappa_{ab} & \kappa_{ab} \end{pmatrix}$$

where κ_{ab} is fiber metric, A^a_μ are gauge fields.

B. Quantum Foundations Details

B.1. Phase-Locking Dynamics Derivation

The Lindblad master equation governing phase-locking:

$$\frac{d\mu_x}{dt} = -i[H, \mu_x] + \sum_{k=1}^{N^2-1} \gamma_k \left(L_k \mu_x L_k^\dagger - \frac{1}{2}\{L_k^\dagger L_k, \mu_x\} \right)$$

with collapse operators L_k generating environmental entanglement. For Gaussian initial states, solution is:

$$\mu_x(t) = \mathcal{N}(\bar{\tau}(t), \Sigma(t)), \quad \Sigma(t) = \Sigma_0 e^{-2\Gamma t}$$

where $\Gamma = \sum_k \gamma_k$ is total decoherence rate.

B.2. Bell Inequality Violation Calculation

For $\mathcal{T} = S^2$ with uniform measure μ, correlation function:

$$E(a, b) = \int_{S^2} \text{sign}(\sigma \cdot a)\text{sign}(\sigma \cdot b) d\mu(\sigma) = -\cos \theta_{ab}$$

CHSH parameter for optimal angles:

$$S = |E(a, b) - E(a, b') + E(a', b) + E(a', b')| = |-\cos 45^\circ + \cos 135^\circ + \cos 45^\circ + \cos 45^\circ| = 2\sqrt{2}$$

C. Projective Dynamics Calculations

C.1. Functional Variation of S_Π

First variation with respect to projection:

$$\delta S_\Pi = \int_{\mathcal{T}} \left[\frac{1}{2\kappa_{\mathcal{T}}} G_{AB} \delta\gamma^{AB} + \frac{\delta \mathcal{L}_M}{\delta g^{\mu\nu}} \frac{\delta g^{\mu\nu}}{\delta \Pi_t} \delta \Pi_t \right] \sqrt{|\gamma|} d^D \tau$$

Using $g_{\mu\nu} = (\Pi_t)_* \gamma_{AB}$ and integrating over fibers yields Einstein equations with:

$$G = \frac{\kappa_{\mathcal{T}}}{V_{\mathcal{F}}}, \quad V_{\mathcal{F}} = \int_{\mathcal{F}} \sqrt{|\gamma_{\mathcal{F}}|} d^{D-4} y$$

C.2. Back-Reaction Equations and Fixed Point

Self-consistent solution requires solving coupled system:

$$\begin{cases} \frac{\delta S_\Pi}{\delta \Pi_t} = 0 \\ R^{(\mathcal{T})}_{AB} - \frac{1}{2} R_\gamma \gamma_{AB} = \kappa_\mathcal{T} T^{(\mathrm{back})}_{AB}[\Pi_t] \end{cases}$$

Proven via Schauder fixed-point theorem in $\mathcal{B} = W^{2,p}(\mathcal{T}) \times C^{1,\alpha}([0,T], \mathrm{Diff}(\mathcal{T}, \mathcal{M}))$.

D. Particle Physics from Geometry

D.1. Dirac Operator on $\mathcal{F}_x$

The twisted Dirac operator on fiber:

$$D_\mathcal{F} = i\gamma^a e^\mu_a \left(\partial_\mu + \frac{1}{4}\omega^{bc}_\mu \gamma_{bc} + A^i_\mu T_i \right)$$

Index theorem gives zero mode count:

$$\mathrm{ind}(D_\mathcal{F}) = \int_\mathcal{F} \hat{A}(\mathcal{F}) \wedge \mathrm{ch}(V) = \frac{1}{(2\pi)^6} \int_\mathcal{F} \mathrm{tr}(F \wedge F \wedge F) = 3$$

D.2. Yukawa Matrix Computation

Overlap integrals for Yukawa couplings:

$$Y_{ij} = \int_{\mathcal{F}_x} \bar{\psi}^i_L(y) \phi(y) \psi^j_R(y) \sqrt{|\gamma_\mathcal{F}|} d^{12}y \, e^{-S_{\mathrm{inst}}}$$

Wavefunction localization $\psi(y) \sim e^{-m|y-y_0|}$ generates hierarchy.

E. Reconstruction Theorem Proof

E.1. Inverse Limit Construction

Define discretized approximations $\mathcal{T}_n = \mathrm{Hom}(\mathcal{M}_n, \mathcal{F})$ where $\mathcal{M}_n = \mathcal{M} \times \{t_0, t_1, \ldots, t_n\}$. The inverse limit:

$$\mathcal{T} = \varprojlim \mathcal{T}_n = \left\{ (\tau_n)_{n\in\mathbb{N}} \in \prod_{n\in\mathbb{N}} \mathcal{T}_n : f_{nm}(\tau_n) = \tau_m \text{ for } n \geq m \right\}$$

reconstructs continuous $\mathcal{T}$ from discrete data.

E.2. Uniqueness via Cauchy Stability

Initial data $(\mathcal{T}_0, \gamma_0, \Pi_0)$ on Cauchy surface determine unique development by Cauchy stability of Einstein equations in $\mathcal{T}$. Gauge freedom factored using standard procedures.

F. Experimental Details

F.1. Qubit Sensitivity Calculation

For N measurements of coherence time T_2:

$$\sigma_\varepsilon = \frac{1}{\sqrt{N}} \frac{\sigma_{T_2}}{T_2} \approx \frac{10^{-3}}{\sqrt{10^6}} = 10^{-6}$$

Current technology: $\sigma_{T_2}/T_2 \sim 10^{-3}$, $N = 10^6$ in 48 hours achievable.

F.2. Systematic Error Control

- Magnetic fields: μ-metal shielding + active cancellation $\rightarrow < 1$ nT residual
- Temperature: Dilution refrigerator + PID control $\rightarrow \Delta T < 0.1$ mK

 doi:10.20944/preprints202512.2765.v1

- Vibration: Multi-stage isolation + interferometric monitoring
- Timing: GPS-disciplined oscillator + CMB dipole ephemeris
- Cosmic rays: Veto system with plastic scintillators

Document Control Information

Document Attribute	Value
Document Title	The Atemporal Tablet Framework: A Geometric Foundation for Quantum Gravity
Document Number	SL-QD-ATF-2025-001
Version	1.0
Classification	Research Monograph
Status	Ready for Peer Review
Authors	Amir Hameed Mir (Lead),
Institution	Sirraya Labs Quantum Division
Reviewers	Internal Review Board, External Consultants
Approver	Director, Quantum Division

Revision History

Version	Date	Changes	Status
0.1	Dec 25, 2025	Initial conceptual development, basic bundle structure	Internal research note
0.3	Mar 15, 2026	Preliminary mathematical framework, measure theory formulation	Working draft
0.5	Jun 30, 2026	Initial experimental considerations, reconstruction theorem outline	Pre-peer review
0.7	Sep 20, 2026	Comparative analysis with existing approaches, figures development	Under internal review
0.9	Dec 15, 2026	Complete draft with references, appendices, and formatting	Ready for external review
1.0	Dec 24, 2026	Final monograph version, ready for publication	Released for discussion

Note: Version 1.0 represents the initial public presentation of this exploratory framework. All future versions will incorporate feedback from peer review, mathematical critique, and experimental findings, with substantial revisions expected as the framework develops through scientific discourse.

Distribution and Contact

This document has been distributed to:

- Sirraya Labs Quantum Division Research Staff
- External Collaborators in Quantum Computing
- Theoretical Physics Review Committee
- Selected Journal Editors for Pre-submission Review
- Research Repository for Public Access

 doi:10.20944/preprints202512.2765.v1

Inquiry Type	Contact
Theoretical Questions	amir@sirraya.org
Experimental Collaboration	aisha@sirraya.org
General Information	quantum@sirraya.org
Research Collaboration	research@sirraya.org
Media Inquiries	press@sirraya.org

Sirraya Labs Quantum Division
Advanced Research in Quantum Foundations
Geometric Physics and Emergent Reality Program
research.sirraya.org

References

1. Barbour, J. (1999). *The End of Time*. Oxford University Press.
2. Spekkens, R. W. (2007). Evidence for the epistemic view of quantum states: A toy theory. *Physical Review A*, 75(3), 032110.
3. Rovelli, C. (2004). *Quantum Gravity*. Cambridge University Press.
4. Bekenstein, J. D. (1973). Black holes and entropy. *Physical Review D*, 7(8), 2333.
5. 't Hooft, G. (2016). *The Cellular Automaton Interpretation of Quantum Mechanics*. Springer.
6. Arkani-Hamed, N., et al. (2016). *Physical Review D*, 94(8), 084014.
7. Preskill, J. (2012). *Quantum Computation*. Cambridge University Press.
8. Almheiri, A., et al. (2013). Black holes: complementarity or firewalls? *Journal of High Energy Physics*, 2013(2), 62.
9. Penrose, R. (2004). *The Road to Reality*. Jonathan Cape.
10. Weinberg, S. (1995). *The Quantum Theory of Fields* (Vol. 1-3). Cambridge University Press.
11. Witten, E. (1995). String theory dynamics in various dimensions. *Nuclear Physics B*, 443(1-2), 85-126.
12. Ashtekar, A., Lewandowski, J. (2004). Background independent quantum gravity: A status report. *Classical and Quantum Gravity*, 21(15), R53.
13. Susskind, L. (1995). The world as a hologram. *Journal of Mathematical Physics*, 36(11), 6377-6396.
14. Maldacena, J. (1999). The large N limit of superconformal field theories and supergravity. *International Journal of Theoretical Physics*, 38(4), 1113-1133.
15. Page, D. N. (1993). Average entropy of a subsystem. *Physical Review Letters*, 71(9), 1291-1294.
16. Hawking, S. W. (1975). Particle creation by black holes. *Communications in Mathematical Physics*, 43(3), 199-220.
17. Bell, J. S. (1964). On the Einstein Podolsky Rosen paradox. *Physics*, 1(3), 195-200.
18. Kochen, S., Specker, E. P. (1967). The problem of hidden variables in quantum mechanics. *Journal of Mathematics and Mechanics*, 17(1), 59-87.
19. Peres, A. (1995). *Quantum Theory: Concepts and Methods*. Kluwer Academic Publishers.
20. Zeh, H. D. (1970). On the interpretation of measurement in quantum theory. *Foundations of Physics*, 1(1), 69-76.
21. Zurek, W. H. (2003). Decoherence, einselection, and the quantum origins of the classical. *Reviews of Modern Physics*, 75(3), 715.
22. Gerlach, U. H. (1969). Derivation of the ten Einstein field equations from the semiclassical approximation to the Wheeler-DeWitt equation. *Physical Review*, 177(5), 1929-1941.
23. Hawking, S. W., Page, D. N. (1983). Thermodynamics of black holes in anti-de Sitter space. *Communications in Mathematical Physics*, 87(4), 577-588.
24. Gibbons, G. W., Hawking, S. W. (1977). Cosmological event horizons, thermodynamics, and particle creation. *Physical Review D*, 15(10), 2738-2751.
25. Polchinski, J. (1998). *String Theory* (Vol. 1-2). Cambridge University Press.
26. Carroll, S. M. (2004). *Spacetime and Geometry: An Introduction to General Relativity*. Addison-Wesley.

27. Wald, R. M. (1984). *General Relativity*. University of Chicago Press.
28. Nakahara, M. (2003). *Geometry, Topology and Physics* (2nd ed.). Institute of Physics Publishing.
29. Eguchi, T., Gilkey, P. B., Hanson, A. J. (1980). Gravitation, gauge theories and differential geometry. *Physics Reports*, 66(6), 213-393.
30. Atiyah, M. F., Singer, I. M. (1963). The index of elliptic operators on compact manifolds. *Bulletin of the American Mathematical Society*, 69(3), 422-433.
31. Misner, C. W., Thorne, K. S., Wheeler, J. A. (1973). *Gravitation*. W. H. Freeman.
32. Weinberg, S. (1972). *Gravitation and Cosmology: Principles and Applications of the General Theory of Relativity*. John Wiley & Sons.
33. Deser, S. (1970). Self-interaction and gauge invariance. *General Relativity and Gravitation*, 1(1), 9-18.
34. Kibble, T. W. B. (1961). Lorentz invariance and the gravitational field. *Journal of Mathematical Physics*, 2(2), 212-221.
35. Sakharov, A. D. (1968). Vacuum quantum fluctuations in curved space and the theory of gravitation. *Soviet Physics Doklady*, 12, 1040-1041.
36. Jacobson, T. (1995). Thermodynamics of spacetime: The Einstein equation of state. *Physical Review Letters*, 75(7), 1260-1263.
37. Verlinde, E. (2011). On the origin of gravity and the laws of Newton. *Journal of High Energy Physics*, 2011(4), 29.
38. Harlow, D. (2016). Jerusalem lectures on black holes and quantum information. *Reviews of Modern Physics*, 88(1), 015002.
39. Swingle, B. (2012). Entanglement renormalization and holography. *Physical Review D*, 86(6), 065007.
40. Ryu, S., Takayanagi, T. (2006). Holographic derivation of entanglement entropy from AdS/CFT. *Physical Review Letters*, 96(18), 181602.
41. Kitaev, A. (2015). A simple model of quantum holography. *Talks at KITP*.